Location of Cholesterol in DMPC Membranes. A Comparative Study by Neutron Diffraction and Molecular Mechanics Simulation†

ARTICLE *in* LANGMUIR · FEBRUARY 2001

Impact Factor: 4.46 · DOI: 10.1021/la001382p

8 AUTHORS, INCLUDING:

Michel Laguerre
Institut Européen De Chimie Et Biologie
166 PUBLICATIONS **2,544** CITATIONS
SEE PROFILE

Wilfrid Neri
Université Bordeaux 1
22 PUBLICATIONS **259** CITATIONS
SEE PROFILE

John Katsaras
Oak Ridge National Laboratory
238 PUBLICATIONS **4,707** CITATIONS
SEE PROFILE

Erick Dufourc
University Bordeaux, CNRS, Bordeaux INP
170 PUBLICATIONS **4,204** CITATIONS
SEE PROFILE

Location of Cholesterol in DMPC Membranes. A Comparative Study by Neutron Diffraction and Molecular Mechanics Simulation†

Alain Léonard,‡ Céline Escrive,§ Michel Laguerre,§ Eva Pebay-Peyroula,|| Willfrid Néri,‡ Tanja Pott,‡ John Katsaras,⊥ and Erick J. Dufourc*,§

Centre de Recherche Paul Pascal, Av. A. Schweitzer, 33600 Pessac, France, Institut Européen de Chimie et Biologie, 33600 Bordeaux-Pessac, France, IBS/UJF, 41 Av. des Martyrs, 37027 Grenoble cedex 1, France, NRC, Stacie Institute for Molecular Sciences Chalk River Laboratories, Chalk River, Ontario K0J 1J0, Canada

Received October 2, 2000. In Final Form: December 29, 2000

The vertical location of 30 mol % cholesterol in a hydrated dimyristoylphosphatidylcholine (DMPC) membrane was determined by neutron diffraction on annealed samples containing deuterated or protonated cholesterol at 10, 20, 25, 30, and 50 °C. The sterol was deuterium-labeled in positions 2, 2, 3, 4, 4, and 6, and proton−deuterium contrast techniques were used to locate the position of the labeled part of the steroid in the membrane. Cholesterol is found well embedded in the membrane, with ring A at 16.3 ± 0.5 Å from the bilayer center at 10 °C. This location linearly decreases to 15.1 ± 0.5 Å at 50 °C, demonstrating that the sterol is not expelled from the membrane on crossing the former gel-to-fluid phase transition of pure DMPC (24 °C). Molecular dynamics were also performed on well-hydrated membranes in the presence and absence of cholesterol. Neutron scattering 1D profiles were then calculated for comparison with experimental neutron scattering data. The profile obtained from pure fluid-phase lipids is in nice agreement both in shape and in bilayer hydrophobic thickness with the experiment. The pure gel-phase calculation leads to the correct line shape but with an overestimated bilayer thickness. In the presence of cholesterol, only the calculation performed with initial gel-phase conditions leads to a hydrophobic thickness in agreement with neutron data. Ring A of cholesterol is found at 15.2 ± 0.5 Å at 10 °C, underestimating the experimental value by only 1 Å. Molecular dynamics show that the hydroxyl group of cholesterol is hydrated and in such a proximity to the carboxyl oxygens of the phospholipids that it can make hydrogen bonds. The ability for molecular dynamics calculations on membranes to determine structural data in membranes is finally discussed.

Introduction

Cholesterol (CH) is found in many biological membranes and is the main sterol of animal organisms. It is equimolar with phospholipids in membranes of liver cells, erythrocytes,[46] and myelin[3] whereas in human stratum corneum, that is, the outermost layer of epidermis, it represents 20 wt % of the lipidic fraction.[8,18] Cholesterol has been extensively studied over the last two decades and is known as a regulator of membrane ordering;[7,19,28,36,43] for a review see ref 53. It has a condensing effect on the lipid acyl chains at a temperature above that of the former gel-to-fluid phase transition of phospholipids and a disordering action below. Using diffraction methods[12,15,49,50] and spectroscopic techniques,[1,7,19,32,41] it has been proposed that cholesterol is located in the membrane. It has further been demonstrated by solid-state NMR that it orients quasi-perpendicularly to the membrane surface and that its

† This work is in memory of Alain Léonard.

* Address correspondence to Erick J. Dufourc, IECB-Polytechnique, FRE CNRS 2247, Av Pey-Berland, BP 108, 33402 Talence cedex, France. Telephone/fax: (33) 5 57 96 22 18. E-mail: erick.dufourc@iecb-polytechnique.u-bordeaux.fr.

‡ Centre de Recherche Paul Pascal.

§ Institut Européen de Chimie et Biologie.

|| IBS/UJF.

⊥ NRC.

(1) Alecio, M. R.; Golan, D. E.; Veatch, W. R.; Rando, R. R. Use of fluorescent cholesterol derivative to measure lateral mobility of cholesterol in membranes. *Proc. Natl. Acad. Sci. U.S.A.* **1982**, *79*, 5171−5174.

(2) Allen, M. P.; Tildesley, D. J. *Computer simulations of liquids*; Clarendon Press: Oxford, 1989.

(3) Ansell, G. B.; Hawthorne, J. N. *Phospholipids*; Plenum Press: Amsterdam, 1964.

(4) Büldt, G.; Gally, H. U.; Seelig, J.; Zaccai, G. Neutron diffraction studies on phosphatidylcholine model membranes. I. Headgroup conformation. *J. Mol. Biol.* **1979**, *134*, 673−691.

(5) Davies, M. A.; Schuster, H. F.; Brauner, J. W.; Mendelsohn, R. Effects of cholesterol on conformational disorder in dipalmitoylphosphatidylcholine bilayers. A quantitative IR study of the depth dependence. *Biochemistry* **1990**, *29*, 4368−4373.

(6) Douliez, J. P.; Léonard, A.; Dufourc, E. J. Conformational approach of DMPC sn-1 versus sn-2 chains and membrane thickness: an approach to molecular protrusion by solid state ^{2}H NMR and neutron diffraction. *J. Phys. Chem.* **1996**, *100*, 18450−18457.

(7) Dufourc, E. J.; Parish, E. J.; Chitrakorn, S.; Smith, I. C. P. Structural and dynamical details of cholesterol-lipid interaction as revealed by deuterium NMR. *Biochemistry* **1984**, *23*, 6063−6071.

(8) Elias, P. M.; Friend, D. S.; Goerke, J. Membrane sterol heterogeneity. Freeze-Fracture detection with saponins and Filipin. *J. Histochem. Cytochem.* **1979**, *27*, 1247−1260.

(9) Faure, C.; Bonakdar, L.; Dufourc, E. J. Determination of DMPC hydration in the L_α and $L_{\beta'}$ phases by ^{2}H solid-state NMR of D_2O. *FEBS Lett.* **1997**, *405*, 263−266.

(10) Faure, C.; Tranchant, J. F.; Dufourc, E. J. Comparative effects of cholesterol and cholesterol sulfate on hydration and ordering of DMPC membranes. *Biophys. J.* **1996**, *70*, 1380−1390.

(11) Fernandez-Puente, L.; Bivas, I.; Mitov, M. D.; Méléard, P. Temperature and chain length effects on bending elasticity of phosphatidylcholine bilayers. *Europhys. Lett.* **1994**, *28*, 181−186.

(12) Franks, N. P. Structural Analysis of Hydrated Lecithin and Cholesterol Bilayers. I. X-ray Diffraction. *J. Mol. Biol.* **1976**, *100*, 345−358.

(13) Gabdoulline, R. R.; Vanderkooi, G.; Zheng, C. Comparison of the structures of dimyristoylphosphatidylcholine in the presence and absence of cholesterol by molecular dynamics simulation. *J. Phys. Chem.* **1996**, *100*, 15942−15946.

(14) Gliss, C.; Randel, O.; Casalta, H.; Sackmann, E.; Zorn, R.; Bayerl, T. Anisotropic motions of cholesterol in oriented DPPC bilayers studied by quasielastic neutron scattering: the liquid-ordered phase. *Biophys. J.* **1999**, *77*, 331−340.

10.1021/la001382p CCC: $20.00
Published on Web 02/14/2001

orientation is temperature independent in the range 15−70 °C.[7,22] The accurate vertical location in the membrane is however a little bit controversial. The pioneering work of Worcerster and Franks[49,50] using 40 mol % [3-$^2H_1$]-cholesterol in egg lecithin showed that carbon-3 of the steroid skeleton was at 18 Å from the bilayer center at room temperature. However, a recent study[34] proposed that cholesterol could be expelled from the bilayer interior at the former gel-to-fluid transition temperature of pure dipalmitoylphosphatidylcholine (DPPC). On the other hand there appears more studies by molecular dynamics of hydrated bilayer systems containing phospholipids and cholesterol. For a review see Berendsen and co-workers,[44] who clearly state the computer perspectives in molecular dynamic studies of lipid bilayers and highlight the difficulties. Among the few works known on simulations of cholesterol-containing systems, one must report those of Gabdouline[13] on a small system, namely 16 dimyristoylphosphatidylcholine (DMPC) molecules and 16 cholesterol molecules in a hydrated bilayer, and of Robinson,[35] who studied an assembly made of 36 DMPC and 4 cholesterol. Calculations were performed for 100 and 400 ps, respectively, but the data were not strictly compared with accurate experimental data. More recently, calculations were carried out for longer times.[29,40,45] The agreement with dynamical experimental data, such as order parameters, was improved, but still there remains experimental facts not accounted for by the calculation. To our knowledge there are no comparisons of structural data, in membrane systems, with molecular dynamics.

In this work we tried to address two main questions: (i) what is the accurate vertical location of cholesterol in the membrane and its possible temperature variation when crossing a former phase transition, and (ii) what is the capability of molecular mechanics to model lipid−cholesterol membrane systems? The first problem was solved by neutron diffraction on oriented samples. We experimentally determined the vertical location of cho-

(15) Hui, S. W. Molecular organization in cholesterol-lecithin bilayers by X-ray and electron diffraction measurements. *Biochemistry* **1983**, *22*, 1159−1164.
(16) Ipsen, J. H.; Mouritsen, O. G.; Bloom, M. Relationships between lipid membrane area, hydrophobic thickness and acyl chain orientational order. (The effects of cholesterol). *Biophys. J.* **1990**, *52*, 405−412.
(17) Katsaras, J.; Raghunathan, V. A.; Dufourc, E. J.; Dufourcq, J. Evidence for a two-dimensional molecular lattice in subgel phase DPPC bilayers. *Biochemistry* **1995**, *34*, 4684−4688.
(18) Lampe, M. A.; Williams, M. L.; Elias, P. M. Human epidermal lipids: characterization and modulations during differentiation. *J. Lipid Res.* **1983**, *21*, 131−140.
(19) Léonard, A.; Dufourc, E. J. Interactions of cholesterol with the membrane lipid matrix. A solid-state NMR approach. *Biochimie* **1991**, *73*, 1295−1302.
(20) Léonard, A.; Milon, A.; Krajewski-Bertrand, M.-A.; Dufourc, E. J. Modulation of Membrane Hydrophobic Thickness by Cholesterol, Cycloartenol and Hopanoid. A Solid State ^{2}H-NMR Study. *Bull. Magn. Reson.* **1993**, *15*, 124−127.
(21) Long, R. A.; Hruska, F.; Gesser, H. D.; Hsia, J. C.; Williams, R. Membrane condensing effect of cholesterol and the role of its hydroxyl group. *Biochem. Biophys. Res. Commun.* **1970**, *41*, 321−327.
(22) Marsan, M. P.; Muller, I.; Ramos, C.; Rodriguez, F.; Dufourc, E. J.; Czaplicki, J.; Milon, A. Cholesterol orientation and dynamics in dimyristoylphosphatidylcholine bilayers: A solid-state deuterium NMR analysis. *Biophys. J.* **1999**, *76*, 351−359.
(23) Marsh, D. *CRC Handbook of Lipid Bilayers*; CRC Press: Boca Raton, FL, 1990.
(24) McIntosh, T. J.; Simon, S. A.; Needham, D.; Huang, C.-H. Interbilayer interactions between sphingomyelin and sphingomyelin/cholesterol bilayers. *Biochemistry* **1992**, *31*, 2020−2024.
(25) McMullen, T. P. W.; McElhaney, R. N. New aspects of the interaction of cholesterol with dipalmitoylphosphatidylcholine bilayers as revealed by high-sensitivity differential scanning calorimetry. *Biochim. Biophys. Acta* **1995**, *1234*, 90−98.
(26) Mohamadi, F.; Richards, N. G. J.; Guida, W. C.; Liskamp, R.; Lipton, M.; Caufield, C.; Chang, G.; Hendrickson, T.; Still, W. C. MacroModel−An integrated software system for modeling organic and bioinorganic molecules using molecular mechanics. *J. Comput. Chem.* **1990**, *11*, 440−467.
(27) Oldfield, E.; Gilmore, R.; Glazer, M.; Gutowsky, H. S.; Hshung, J. C.; Kang, S. Y.; King, T. S.; Meadows, M.; Rice, D. Deuterium nuclear magnetic resonance investigation of the effects of proteins and polypeptides on hydrocarbon chain order in model membrane systems. *Proc. Natl. Acad. Sci. U.S.A.* **1978**, *75*, 4657−4660.
(28) Oldfield, E.; Meadows, M.; Rice, D.; Jacobs, R. Spectroscopic studies of specifically deuterium labeled membrane systems. Nuclear magnetic resonance investigation of the effects of cholesterol in model systems. *Biochemistry* **1978**, *17*, 2727−1739.
(29) Pasenkiewicz-Gierula, M.; Rog, T.; Kitamura, K.; Kusumi, A. Cholesterol effects on the phosphatidylcholine bilayer polar region: a molecular simulation study. *Biophys. J.* **2000**, *78*, 1376−1379.
(30) Pebay-Peyroula, E.; Dufourc, E. J.; Szabo, A. G. Location of diphenyl-hexatriene and trimethylammonium-diphenyl-heaxtriene in dipalmytoylphosphatidylcholine bilayers by neutron diffraction. *Biophys. Chem.* **1994**, *53*, 45−56.
(31) Pfeiffer, W.; Henkel, T.; Sackmann, E.; Knoll, W.; Richter, D. Local dynamics of lipid bilayers studied by incoherent quasielastic neutron scattering. *Europhys. Lett.* **1989**, *8*, 201−206.
(32) Pott, T.; Maillet, J. C.; Dufourc, E. J. Effects of pH and cholesterol on DMPA membranes: a solid state ^{2}H- and ^{31}P-NMR study. *Biophys. J.* **1995**, *69*, 1897−1908.
(33) Rand, R. P.; Parsegian, V. A. Hydration forces between phospholipid bilayers. *Biochim. Biophys. Acta* **1989**, *988*, 351−376.
(34) Reinl, H.; Brumm, T.; Bayerl, T. M. Changes of the physical properties of the liquid-ordered phase with temperature in binary mixtures of DPPC with cholesterol. *Biophys. J.* **1992**, *61*, 1025−1035.
(35) Robinson, A. J.; Richards, W. G.; Thomas, P. J.; Hann, M. M. Behavior of cholesterol and its effect on headgroup and chain conformation in lipid bilayers: a molecular dynamics study. *Biophys. J.* **1995**, *68*, 164−170.
(36) Sankaram, M. B.; Thompson, T. E. Modulation of phospholipid acyl chain order by cholesterol. A solid state ^{2}H nuclear magnetic resonance study. *Biochemistry* **1990**, *29*, 10676−10684.
(37) Saxena, A. M.; Schoenborn, B. P. Correction factors for neutron diffraction from lamellar structures. *Acta Crystallogr.* **1977**, *A33*, 813−818.
(38) Schultz, G. E.; Schirmer, R. H. *Principles of protein structure;* Springer-Verlag: New York, 1979.
(39) Smith, G. S.; Sirota, E. B.; Safinaya, C. R.; Clark, N. A. Structure of the L_β phases in a hydrated phosphatidylcholine multimembrane. *Phys. Rev. Lett.* **1988**, *60*, 813−816.
(40) Smondyrev, A. M.; Berkowitz, M. L. Molecular dynamics simulation of dipalmitoylphosphatidylcholine membrane with cholesterol sulfate. *Biophys. J.* **2000**, *78*, 1672−1680.
(41) Smutzer, G. A fluorescent sterol probe study of cholesterol/phospholipid membranes. *Biochim. Biophys. Acta* **1988**, *946*, 270−280.
(42) Stockton, G. W.; Polnaszek, C. F.; Tulloch, A. P.; Hasan, F.; Smith, I. C. P. Molecular Motion and Order in Single Bilayer Vesicles and Multilamellar Dispersions of Egg Lecithin and Lecithin-Cholesterol Mixtures. A Deuterium Nuclear Magnetic Resonance Study of Specifically Labeled Lipids. *Biochemistry* **1976**, *15*, 955−966.
(43) Taylor, M. G.; Smith, I. C. P. The conformations of nitroxide-labeled fatty acid probes of membrne structure as studied by 2 H-NMR. *Biochim. Biophys. Acta* **1983**, *733*, 256−263.
(44) Tieleman, D. P.; Marrink, S. J.; Berendsen, H. J. A computer perspective of membranes molecular dynamics studies of lipid bilayer systems. *Biochim. Biophys. Acta* **1997**, *1331*, 235−270.
(45) Tu, K.; Klein, M. L.; Tobias, D. J. Constant-pressure molecular dynamics investigation of cholesterol effects in a dipalmitoylphosphatidylcholine bilayer. *Biophys. J.* **1998**, *75*, 2147−2156.
(46) Van Deenen, L. L. M.; De Gier, J. *The Red Blood Cell*; Academic Press: New York, 1964.
(47) Vist, M. R.; Davis, J. H. Phase equilibria of cholesterol dipalmitoylphosphatidylcholine mixtures: ^{2}H-nuclear magnetic resonance and differential scanning calorimetry. *Biochemistry* **1990**, *29*, 451−464.
(48) Weisz, K.; Gröbner, G.; Mayer, C.; Stohrer, J.; Kothe, G. Deuteron nuclear magnetic resonance study of the dynamic organization of phospholipid/cholesterol bilayer membranes: molecular properties and viscoelastic behavior. *Biochemistry* **1992**, *31*, 1100−1112.
(49) Worcester, D. L. Neutron Beam Studies of Biological Membranes and Membrane Components. In *Biological Membranes*; Chapman, D., Wallach, D. F. H., Eds.; Academic Press: London, 1976; Vol. 3, pp 1−46.
(50) Worcester, D. L.; Franks, N. P. Structural Analysis of Hydrated Egg Lecithin and Cholesterol Bilayers. II Neutron Diffraction. *J. Mol. Biol.* **1976**, *100*, 359−378.
(51) Worcester, D. L.; Kaiser, H.; Kulasekere, R.; Torbet, J. Phase determination and contrast variation methods in neutron diffraction studies of biological lipids. *Inverse problems in scattering and imaging*; SPIE: Washington, DC, 1992; pp 451−456.
(52) Wu, Y.; He, K.; Ludtke, S. J.; Huang, H. W. X-ray diffraction study of lipid bilayer membranes interacting with amphiphilic helical peptides: diphytanoyl phosphatidylcholine with alamethicin at low concentrations. *Biophys. J.* **1995**, *68*, 2361−2369.
(53) Yeagle, P. L. Cholesterol and the cell membrane. *Biochim. Biophys. Acta* **1985**, *822*, 267−287.

lesterol in DMPC bilayers by performing neutron diffraction experiments at 10, 20, 25, 30, and 50 °C on samples containing either deuterated or protonated cholesterol. This was accomplished by taking advantage of the difference in sign and magnitude of the scattering amplitudes of these two isotopes. The difference between both Fourier profiles indeed allows us to extract distances of the body-labeled cholesterol from the bilayer center, as has been done for a number of phospholipids.[4,55] Problem ii was addressed by comparing neutron structural data to molecular mechanics simulations carried out for 2−3 ns on a cholesterol-containing DMPC membrane in water, under conditions very close to those of neutron diffraction experiments. The molecular dynamics data were used to reconstruct the neutron scattering 1D profile to provide direct comparison with experimental data. Because the gel- or fluid-phase nature of the membrane in its initial state was found to be important, molecular mechanics were also performed on pure phospholipid gel- or fluid-phase membranes and compared with neutron data.

Materials and Methods

Chemicals. DMPC was purchased from Interchim (Montluçon, France) whereas cholesterol was purchased from Sigma Chemical Co. (St Louis, MO). Deuterium-labeled cholesterol in carbon positions 2, 2, 3, 4, 4, and 6 was synthesized according to already published procedures.[7] Heavy water (D_2O) was obtained from ILL (Grenoble, France). The purities of DMPC and cholesterol were checked by thin-layer chromatography prior to and after completion of experiments; little degradation (less than 5%) was detected.

Sample Preparation. Oriented multilayers were prepared as follows. Mixtures of DMPC (30 mg) with cholesterol were cosolubilized in chloroform/methanol (2/1 v/v). Microscope slides (previously treated by overnight immersion in a chromic acid solution, washed, and dried) were coated with this organic solution and placed in an oven at 50 °C for 3 h to ensure evaporation. Sample hydration and annealing were achieved by placing the slides in the presence of a saturated KCl solution in the oven at 50 °C for 3 h. This solution ensures a constant relative humidity of 85%. This procedure was repeated for samples containing protonated or deuterated cholesterol. To determine the sign of the structure factors (vide infra), the samples were also studied with different amounts of H_2O/D_2O mixtures (0, 50, 100% D_2O); that is, samples were dehydrated in the oven (50 °C, 4−5 h) and subsequently equilibrated with the desired H_2O/D_2O mixture, as described above.

Neutron Diffraction. Samples were mounted on a goniometer placed in a sealed temperature-controlled aluminum can in the presence of an appropriate saturated KCl bath to maintain constant relative humidity at all temperatures studied. Diffraction experiments were performed on the D16 diffractometer at the Institut Laue-Langevin (ILL, Grenoble, France) and the V1 diffractometer at the Berlin Neutron Scattering Center (BENSC, Berlin, Germany), respectively operating at $\lambda = 4.525$ and 5.8 Å. Data collection was accomplished as described by Pebay-Peyroula.[30] Bragg peaks were separated by more than 3.5° in 2θ and therefore did not overlap. The stronger reflections could be measured in minutes whereas the weaker ones were scanned for several hours to get a good signal-to-noise ratio. The signal coming from the wires on the periphery of the detector was perturbed and not taken into account (a mask was created). Intensities on the detector surface were corrected from the background signal (water scan). Linear regrouping was performed by running ILL-made software (HPSD16), hence affording peak intensities $I(h)$ as a function of 2θ with h standing for the order of the diffraction. Sample mosaicity, η, was measured from so-called rocking curves[37,55] and ranged between 1 and 2°, demonstrating the high degree of orientation of our samples. Further treatment according to equations developed in the Appendix was accomplished on VAX computer systems according to unpublished FORTRAN programs (E. J. Dufourc and E. Pebay-Peyroula).

Molecular Mechanics Simulation. Calculations were performed running Macromodel version 5.0 on a SGI Indy 4400SC workstation (Columbia University, NY[26]) and Insigth II and Discover version 97 (Molecular Simulations Inc.) on a quadriprocessor SGI Origin 200 server. To set up the bilayer model, DMPC and cholesterol molecules were at first built in Macromodel and minimized using the MM2* force field (1987 parameters). For DMPC, all the torsional angles derived from the X-ray structure of DMPC·$2H_2O$ were then applied to the previous structure. For cholesterol, the X-ray structure was directly used after steepest descent minimization in order to ensure a "quasi-ideal" conformation. The lipids were then imported into InsightII, submitted to a MOPAC/MNDO charge calculation, and partitioned into neutral groups. A 13 Å group-based cutoff was used throughout the calculations. A hexagonal crystalline bilayer of 2×30 DMPC was built at first, roughly minimized, and inserted at the center of a $40 \times 80 \times 29$ Å^3 box (volume of 92 800 Å^3, $S_{lip} = 39$ Å^2). The bilayer was soaked with water, fully minimized, and submitted to a 150 ps molecular dynamics run with volume kept constant. The resulting DMPC molecules were then used as a "premelted" lipids database. They were set randomly on a hexagonal lattice, leading to a specific surface of 63 Å^2 with an initial P···P distance across the bilayer of 36 Å. All severe van der Waals contacts were removed by hand, and this assembly was taken as a template for all fluid-phase simulations in the absence and presence of cholesterol.

(i) Fluid-Phase DMPC Simulation. The above template was then centered in a $42.5 \times 60.0 \times 44.4$ Å^3 box, soaked with water (21.5 H_2O/lipid) for a total amount of 10 947 atoms, treated with periodic boundary conditions, and thoroughly minimized using a conjugate gradient method (12 000 cycles, final rms of 2×10^{-3}). The resulting system was then submitted to a molecular dynamics run with the following conditions: temperature of 320 K, time step = 1.5 fs, group cutoff of 13 Å, snapshots stored every 1 ps, 500 ps at constant volume, and then 2 ns at constant pressure.

(ii) Cholesterol-Containing Membrane Simulation with Initial Fluid Phase Conditions. One-third of the phospholipids of the above-mentioned template were removed and replaced by 20 cholesterol molecules in a way to avoid sterol clusters and to position the hydroxyl group close to DMPC carboxylates. The resulting bilayer was then placed in the center of a $42.5 \times 60.0 \times 44.4$ Å^3 box and soaked with water (namely 1027 molecules); then the whole assembly (9281 atoms) was treated with periodic boundary conditions and thoroughly minimized using a conjugate gradient method (13 000 cycles, final rms of 7×10^{-4}). The resulting system was then submitted to a molecular dynamics run (CVFF force field (Discover 95)) with the following starting conditions: constant pressure, temperature of 283 K, time step = 1.5 fs, group cutoff of 13 Å, snapshots stored every 1 ps and for a total calculation time of 2 ns.

(iii) Gel-Phase DMPC Simulation. A hexagonal lattice of 2×30 DMPC was built with an initial specific surface of 50.1 Å^2 and with a starting P···P distance across the bilayer of 37 Å. The resulting bilayer was then placed in the center of a $38.0 \times 66.0 \times 39.6$ Å^3 box and soaked with water (1029 molecules, i.e. 17.15 H_2O/lipid). The whole assembly (10 167 atoms) was then treated with periodic boundary conditions and thoroughly minimized using a conjugate gradient method (12 000 cycles, final rms of 3×10^{-3}). As above, the resulting system was then submitted to a molecular dynamics run with the following conditions: temperature of 278 K, time step = 1.5 fs, group cutoff of 13 Å, snapshots stored every 1 ps, 250 ps at constant volume, and then 2 ns at constant pressure.

(iv) Cholesterol-Containing Membrane Simulation with Initial Gel-Phase Conditions. The starting template was the initial bilayer of the above system (gel phase) in which one-third of the phospholipids had been removed and replaced by 20 cholesterol molecules in such a way that clusters were avoided and sterol hydroxyl groups placed close to DMPC carboxylates. The resulting bilayer was centered in a $38.0 \times 60.0 \times 39.6$ Å^3 box and soaked

(54) Zaccai, G.; Blasie, J. K.; Schoenborn, B. P. Neutron Diffraction Studies on the Location of Water in Lecithin Bilayer Model Membranes. *Proc. Natl. Acad. Sci. U.S.A.* **1975**, *72*, 376−380.

(55) Zaccai, G.; Büldt, G.; Seelig, A.; Seelig, J. Neutron diffraction studies on phosphatidylcholine model membranes. II. Chain conformation and segmental disorder. *J. Mol. Biol.* **1979**, *134*, 693−706.

with water (779 molecules). The whole assembly (8537 atoms) was then treated with periodic boundary conditions and thoroughly minimized using a conjugate gradient method (10 000 cycles, final rms of 6×10^{-3}). As above, the resulting system was then submitted to a molecular dynamics run with the following conditions: temperature of 283 K, time step = 1.5 fs, group cutoff of 13 Å, snapshots stored every 1 ps, 200 ps at constant volume, and then 3 ns at constant pressure.

Calculation of Neutron Density Profiles from Molecular Dynamics. The atomic *x*, *y*, *z* coordinates of all atoms coming from the simulation were used to calculate the one-dimensional density profile in a direction normal to the membrane plane. The amplitude of diffraction of atom *i* at position x_i onto the bilayer normal was described by a Gaussian function:

$$a_i(x) = \frac{b_i}{\sigma\sqrt{2\pi}} \, e^{-(x-x_i)^2/2\sigma^2}$$

where b_i is the coherent scattering amplitude (Fermi amplitude) and σ the Fermi width. b_i values for all isotopes in membranes can be found in ref 49 and are reproduced below for atoms of interest in our study: $b_i(\mathrm{H}) = -0.374 \times 10^{-12}$ cm, $b_i(\mathrm{D}) = 0.667 \times 10^{-12}$ cm, $b_i(\mathrm{C}) = 0.664 \times 10^{-12}$ cm, $b_i(\mathrm{O}) = 0.580 \times 10^{-12}$ cm, $b_i(\mathrm{N}) = 0.936 \times 10^{-12}$ cm, $b_i(\mathrm{P}) = 0.510 \times 10^{-12}$ cm. The one-dimensional density profile of the membrane is obtained by summing up a_i for all atoms of the molecular mechanics calculation. To account for cholesterol selective deuteration, the protons of interest were exchanged by deuterons in the coordinates file. The procedure (E. Dufourc, unpublished) was written in FORTRAN using the Absoft Pro Fortran package (Rochester Hills, USA) and run on a personal computer.

Theoretical Background on Neutron Diffraction

The aim of such neutron diffraction experiments is to reconstruct the one-dimensional neutron scattering profile of the membrane by Fourier transformation of the structure factors, $F(h)$. Intensities of Bragg peaks are the observables from which $F(h)$ values are obtained by performing suitable corrections to account for experimental setup. The absolute values of the structure factors can be expressed as

$$|F(h)| = (L_1(h)\, L_2(h)\, L_3(h))^{-1/2} I(h)^{1/2} \qquad (1)$$

where $L_i(h)$ are correction factors related to the experimental setup and to sample geometry (see the Appendix). Because the sample structure is centrosymmetric, the sign of the structure factor is ±1. It can be determined from the linear dependence of the neutron structure factor, for a given order *h*, versus the D_2O water content in the water layer.[50] Two methods for sign determination are presented in the Appendix.

The Fourier expression for the coherent scattering amplitude density of the membrane, in real space, is written as[4,30,49]

$$\rho(x) = \frac{2}{d} \sum_{h=1}^{h_{\max}} F(h) \cos\left(\frac{2\pi h x}{d}\right) \qquad (2)$$

where *x* is the direction normal to the bilayer surface and *d* the lamellar repeat spacing. When experiments are performed with protonated and deuterated molecules embedded in the bilayer, the scattering profile of the labeled position is obtained from the difference between profiles obtained with labeled and unlabeled molecules:[30]

$$\rho_{\mathrm{label}}(x) = \frac{2}{d} \sum_{h=1}^{h_{\max}} [F^{\mathrm{D}}(h) - sF^{\mathrm{H}}(h)] \cos\left(\frac{2\pi h x}{d}\right) \qquad (3)$$

where *s* is an appropriate scaling factor. $F^{\mathrm{D}}(h)$ and $F^{\mathrm{H}}(h)$, respectively, represent the structure factors for membranes containing the deuterated and protonated molecule. Absolute scaling can be obtained from the water distribution profiles.[30,54]

Results

Structure Factors. Diffraction patterns were recorded for DMPC bilayers containing 30 mol % protonated or deuterated cholesterol. Samples in the absence of cholesterol were also investigated. Each sample was examined for three D_2O concentrations (0, 50, and 100%, v/v) and several temperatures (10, 20, 25, 30, and 50 °C). Pure DMPC membranes were only examined at 10 and 50 °C. When changing temperature or D_2O content, $\theta-2\theta$ scans were performed until no further change in intensity and 2θ position was observed in the diffraction patterns. In some cases, waiting for equilibrium could last up to 12 h. Significant Bragg peak intensities could be observed up to the tenth order, depending on membrane composition and/or temperature. The lamellar repeat distance was obtained from a least-squares fit of the Bragg law applied to all detectable orders ($d = h\lambda/2 \sin\theta_B$, θ_B standing for the Bragg diffraction angle; Table 1). It can be noted that, for a given temperature, *d* values are the same within 0.3 Å for systems containing labeled or unlabeled molecules. For a given sample and temperature, H_2O-D_2O exchange did not induce modifications in *d* greater than 0.1 Å (data not shown). As a general comment, it is noted that the presence of cholesterol leads to a *d* increase of 3.3 ± 0.1 Å at 10 °C and 4.2 ± 0.1 Å at 50 °C. The thermal variation over 40 °C leads to a decrease of the lamellar repeat distance by 5.8 ± 0.1 and 6.7 ± 0.1 Å, respectively, in the presence and absence of cholesterol.

Structure factors were calculated as described in the Theoretical Background on Neutron Diffraction and Appendix sections. The signs of $F(h)$ up to $h = 5$ were determined using H_2O-D_2O exchange and methods A or B described in the Appendix. Such a contrast procedure could not be performed for $h > 5$ due both to weak signals and to time limitations on the neutron lines. In this case, signs were successively varied and Fourier profiles calculated. A criterion of choice was a close coincidence with scattering profiles already published in the literature. All results are collected in Table 1. One clearly remarks that differences markedly occur for systems containing labeled and unlabeled cholesterol molecules.

Membrane Profiles in the Presence and Absence of Cholesterol. Equation 2 was used together with $F(h)$ and *d* values from Table 1 to calculate the one-dimensional coherent scattering amplitude density of the membrane, in the presence and absence of cholesterol at 10 (Figure 1B) and 50 °C (Figure 1A). Profiles in the absence of sterol (dashed lines) are in good agreement with similar ones obtained with DMPC or DPPC molecules.[49,50,55] In particular the glyceroester regions are recognized as the two most intense peaks[4] on each side of the bilayer center and the bilayer hydrophobic thickness, d_h, can be measured from this peak-to-peak distance. The temperature variation of the smectic repeat distance *d* and of d_h, for cholesterol-containing systems, is reported in Figure 2. One remarks that the membrane hydrophobic thickness only diminishes by 2.0 ± 0.5 Å from 10 to 50 °C, whereas *d* decreases by about 6 Å. The same is also observed in the absence of cholesterol (Figure 1 and Table 1).

Difference Profiles Obtained from Labeled and Unlabeled Cholesterol-Containing Systems. The labeled positions of cholesterol are obtained by using eq 3, that is, by noting differences between structure factors

Table 1. Temperature Dependence of Experimental Structure Factors for DMPC and 30 mol % Cholesterol−DMPC[a]

	30 mol % cholesterol−DMPC											
	10 °C		20 °C		25 °C		30 °C		50 °C		DMPC	
h	H	D	H	D	H	D	H	D	H	D	10 °C	50 °C
1	−269	−305	−202		−291	−322	−211	−266	−337	−377	−295	−363
2	−449	−600	−225		−177	−277	−184	−270	−339	−471	−400	−427
3	+330	+390	+183		+190	+280	+183	+255	+298	+396	+403	+380
4	−158	−69	−111		−144	−125	−131	−106	−195	−138	−120	−94
5	−108	−192	−25		−49	−109	0	−81	−60	−161	−200	−103
6	−21	−45	0		0	0	0	0	0	0	−51	−52
7	+33	+113	0		0	+70	0	+52	+40	+104	+105	+49
8	−41	−40	−54		−66	−72	−65	−70	−107	−125	−41	
9	−36	−106									−159	
10											+56	
d (Å)	57.9	57.6	55.3		54.7	54.7	53.7	54.0	51.8	52.0	54.4	47.7

[a] The left column (H) under each temperature stands for systems containing unlabeled cholesterol whereas the right column (D) is for deuterium-labeled cholesterol-containing systems. *h* is the diffraction order and *d* the smectic repeat distance. The accuracy in *F* ranges from 5% (large *F* values) to 15% (low *F* values). The accuracy in *d* is ±0.1 Å.

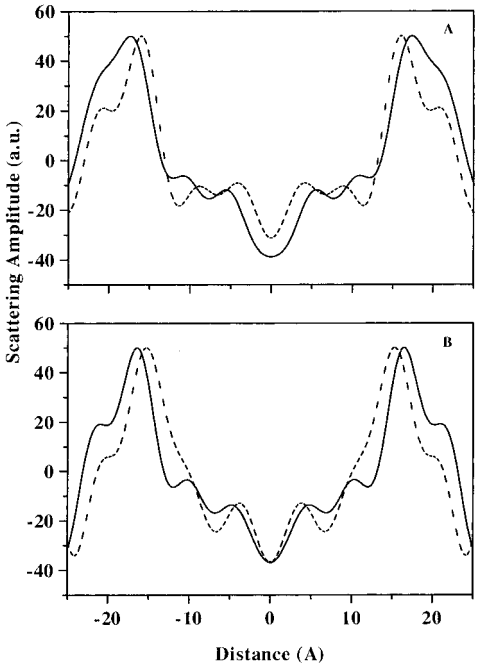

Figure 1. One-dimensional neutron scattering amplitude density of the membrane, in the presence (solid line) and absence (dashed line) of cholesterol at 10 (A) and 50 °C (B). Profiles are arbitrarily normalized to the most intense peak for easiness in comparison and were calculated with eq 2 of the text. The bilayer center is set at 0 Å.

obtained with deuterated and undeuterated systems (Table 1, columns D and H) and then performing the cosines Fourier transformation. A typical example of the resulting deuterated cholesterol Fourier profile (bold line) is plotted in Figure 3C together with the bilayer profile in the presence of cholesterol (thin line). Although there are small undulations due to truncation errors in the Fourier transformation, two major peaks are clearly identified at ±16 Å from the bilayer center. This clearly indicates that cholesterol is well inside the hydrophobic bilayer interior. The six deuterons that are very close in the rigid molecular structure of cholesterol are not resolved due to the limited number of orders (8) to perform the Fourier transformation. Only an envelope of ∼4 Å width at half-maximum is obtained. The peak-to-peak separation between maxima in the Fourier profile of labeled cholesterol, d_c, was measured by fitting the major peaks in real space by a Gaussian function. To prevent systematic errors due to truncation when performing Fourier transformation with few orders, a fit in the reciprocal space was also performed according to the procedure introduced by Büldt and co-workers.[4] Both fitting procedures led to the same result within ±0.1 Å. The resulting data, that is, the distance, d_c, between the barycenters of the six cholesterol deuterons located on each of the two membrane monolayers, are plotted as a function of temperature in Figure 2. A small linear decrease of 2 ± 0.5 Å is observed on going from 10 to 50 °C and parallels that of the hydrophobic bilayer thickness, d_h. d_c is always smaller by 2−3 Å than d_h, in the temperature range of our study.

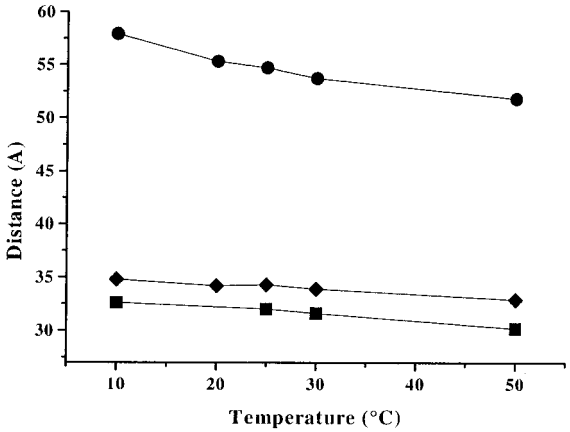

Figure 2. Temperature dependence of the smectic repeat distance, *d* (●), membrane hydrophobic thickness, d_h (◆), and peak-to-peak separation, d_c (■). d_h is measured between the most intense peaks in the Fourier neutron scattering profiles of DMPC containing 30 mol % cholesterol whereas d_c is obtained from the Fourier difference profiles of systems containing labeled and unlabeled cholesterol (see text). The accuracies in the measured distances are ±0.5 Å (◆, ■) and ±0.1 Å (●).

Molecular Mechanics Simulation on Pure Phospholipid Systems. To evaluate the capability of molecular mechanics to give a structural representation of the membrane system, calculations were performed with a bilayer composed of 60 DMPC molecules and 1029 and 1289 water molecules for gel- and fluid-phase conditions, respectively. Under such conditions the membrane has been shown to be well hydrated[9] in both the $L_{\beta'}$ and L_α phases. At the end of a 2 ns run the one-dimensional scattering profiles were calculated from the atomic coordinates as described in the Materials and Methods. The resulting profiles are shown in Figure 4 (dashed lines) together with the corresponding profiles coming from neutron scattering. Two remarks must be made. First, the neutron experimental profile in the fluid phase was

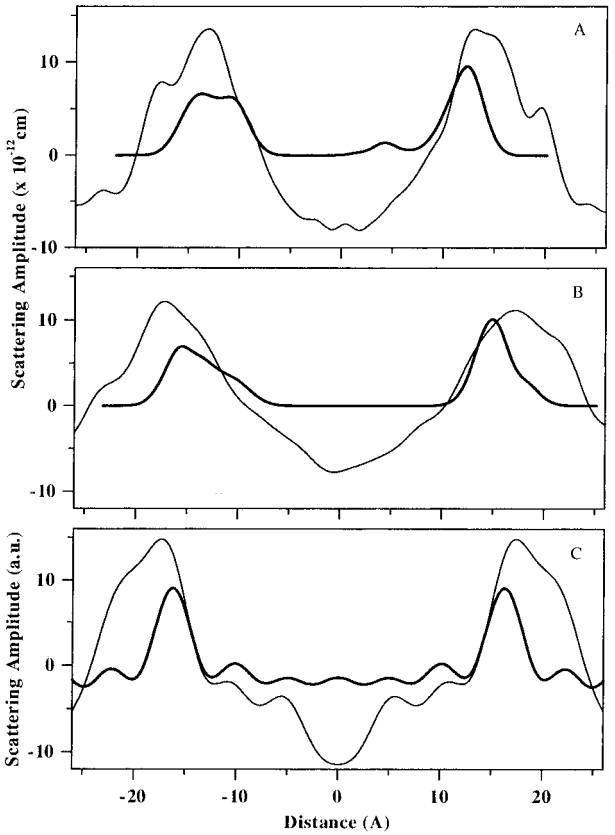

Figure 3. One-dimensional neutron scattering amplitude density of [2,2,3,4,4,6-$^2H_6$]cholesterol (solid bold line) embedded in a DMPC membrane (solid thin line): (C) from experimental neutron data using eqs 2 and 3 of the text; (B) from a 3 ns molecular mechanics simulation under gel-phase starting conditions (see text); (A) from a 2 ns molecular mechanics simulation under fluid-phase starting conditions.

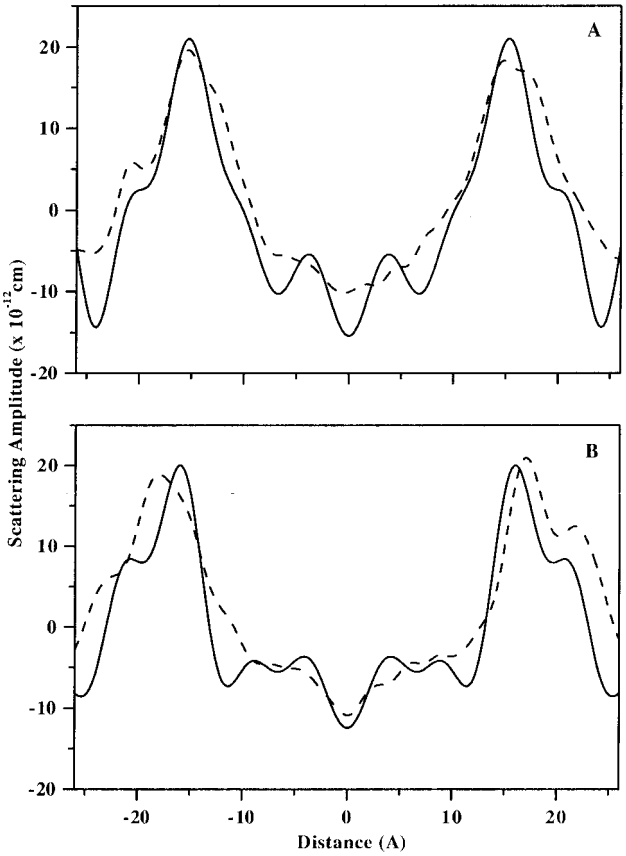

Figure 4. One-dimensional neutron scattering amplitude density of DMPC membranes in gel (panel B) and fluid phases (panel A). Solid lines show profiles from experimental neutron data whereas dashed lines come from a 2 ns molecular mechanics simulation (see text for details).

obtained from 7 Bragg peaks whereas 10 orders were used for the gel phase (see Table 1). This means that there are less truncation errors in the cosines Fourier transformation of the gel-phase profile. Second, the calculation of the neutron profile with molecular mechanics coordinates was performed with a Fermi width (σ) of 1 Å. Such a width was found necessary to compensate for the limited number of lipids that constitute the bilayer. Although the number of atoms is quite important for the calculation (about 10 000), their limited number also leads to nonsymmetrical profiles for the two monolayers (see dashed curves). Following the two above comments, it is only necessary to focus on the dominant features in comparing profiles coming from experiments and from calculation. For fluid-phase conditions, both the neutron data and the molecular dynamics are in good agreement. The major peaks that reflect the hydrophobic thickness are almost on top of each other and lead to a d_h of 30.8 ± 0.5 and 30.1 ± 0.5 Å, respectively. The gel-phase profiles (Figure 4B) are in fair agreement. The depth in the bilayer center, which is due to the presence of end chain CH_3 groups, is found in both profiles. The structure of the major peaks, that is, the glycero-ester region and the phosphocholine headgroup, is also seen in both curves. However, the bilayer hydrophobic thickness, d_h, is greater for the simulation (35.0 ± 0.5 Å) than for the experimental data (32.2 ± 0.5 Å).

The result of the molecular dynamics runs may also be visualized by representing the membrane in a pseudo all-atom display. Figure 5A and B represents the "upper" monolayer that corresponds to positive distances in Figure 4. For clarity, the hydrogen atoms of the lipids are not shown. The phosphorus atoms are represented by orange spheres whereas the carbonyl oxygens of the glyceroester moiety are depicted with pink balls. It can be clearly seen that phosphorus atoms are better separated from the glyceroester region in the gel rather than in the fluid phase, as was also seen on the neutron scattering profiles. Some additional interesting geometrical and dynamical parameters can be extracted from the various simulated phases (full details on fluid phases will appear in another paper in preparation). The specific lipid surface reaches an equilibrium value of 61.03 ± 0.15 Å^2 for the fluid phase and 49.45 ± 0.15 Å^2 for the gel phase. Concerning the lateral diffusion parameters, calculated values are respectively 8.80 × 10^{-8} cm^2/s for the lipid headgroup and 17.0 × 10^{-8} cm^2/s for the entire lipid in the DMPC fluid phase. For gel-phase DMPC, the simulation leads to 2.10 × 10^{-8} cm^2/s for polar headgroups and 7.10 × 10^{-8} cm^2/s for the whole lipid. It must be indicated here that self-diffusion coefficients are obtained with the Insight II computing package, following Einstein's equation: one-sixth of the slope of the mean square displacement versus time.[2] It is important to note that this equation has been derived for isotropic motions and is valid provided that the correlation time for a given diffusive motion is much smaller that the time frame of the entire molecular dynamics calculation. Hence, in some of our simulations we may reach the validity limit of diffusion parameter calculations from Insight II.

Molecular Mechanics Simulation on Cholesterol–Phospholipid Systems. The vertical location of cholesterol was also addressed by molecular dynamics. As

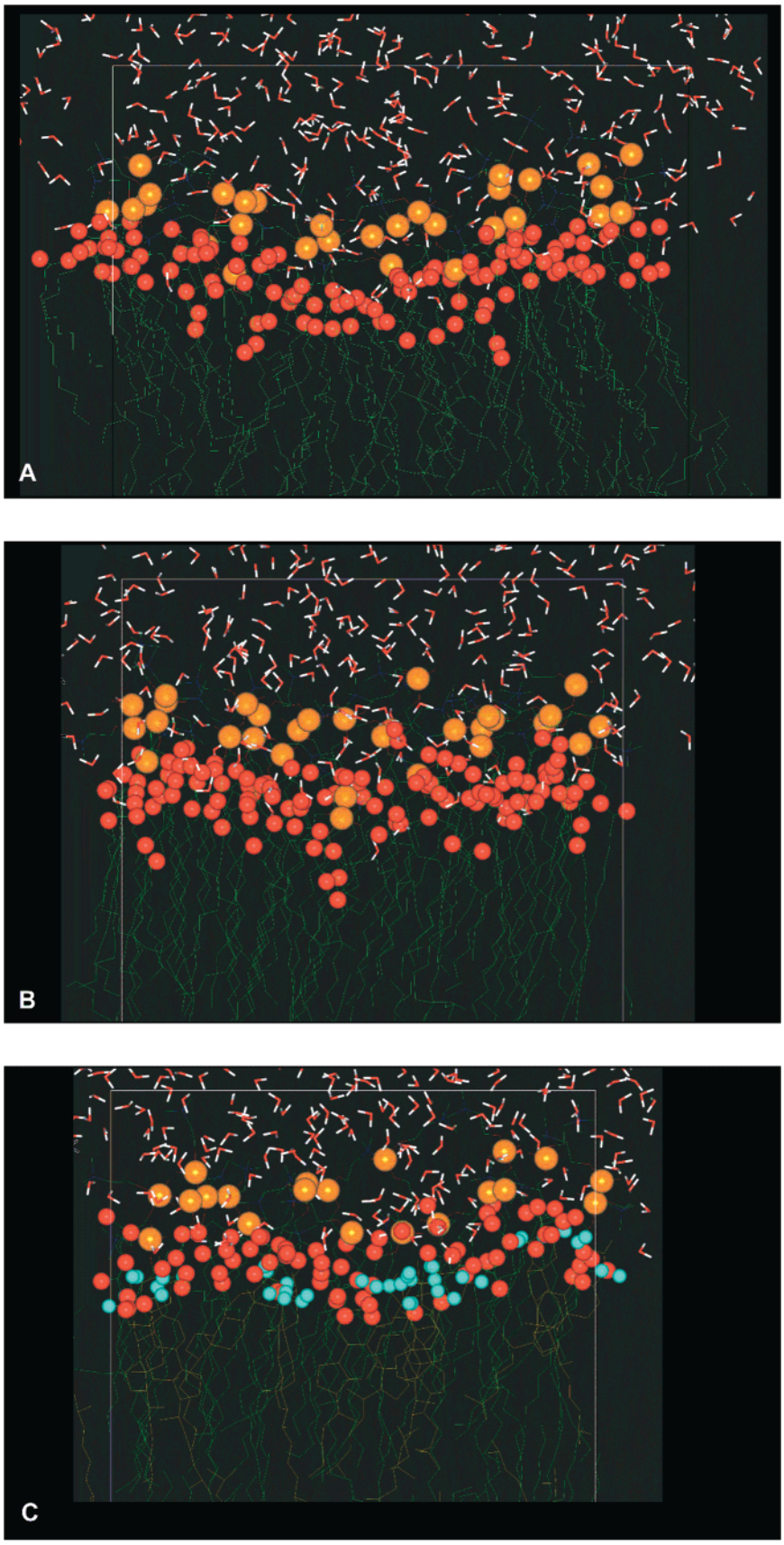

Figure 5. Snapshot representation of the DMPC fluid phase (A) after a 2 ns run, of the DMPC gel phase (B) after a 2 ns run, and of the DMPC−cholesterol system (C) after a 3 ns molecular dynamics run. For clarity, only one bilayer leaflet, that corresponding to positive distances in neutron scattering profiles, is shown and the hydrogen atoms have been removed from the lipids. For a better reading of the figure, some atoms are highlighted by spheres with the following color code: ester oxygens of the two phospholipid fatty acyl chains in red, phosphorus atoms in orange, and the six cholesterol deuterons (positions 2, 2, 3, 4, 4, and 6) in blue. The water molecules are depicted as white−red sticks, and the carbon chain structure is depicted in shadowed green.

indicated in the Materials and Methods, 20 phospholipids were exchanged by cholesterol molecules in such a way that, in the initial state, all sterols were positioned with their hydroxyl group close to the water interface. Two simulations were performed with very different initial conditions: the first one, in which the phospholipids were taken in their fluid state, and another one, in which the gel state was considered as a starting point. After energetic minimization and dynamical treatment for respectively 2 and 3 ns, a final state was attained and the one-dimensional scattering profiles were calculated from the atomic coordinates. The resulting profiles are shown in Figure 3A and B. The entire membrane is shown in thin lines whereas the cholesterol deuterons at positions 2, 2, 3, 4, 4, and 6 are represented by a bold line. The same remarks concerning the finite size of the molecular dynamics box, as already mentioned above, may be made here. As a consequence, asymmetry in the calculated scattering profile appears both for the membrane and for the cholesterol deuterons. On comparing to neutron scattering experimental data (Figure 3C), one sees that the bilayer center showing negative scattering amplitude (CH_3 groups of lipid and cholesterol) is seen in both parts A and B of Figure 3. However, it clearly appears that Figure 3B is much closer to the experimental data (Figure 3C) than the figure calculated from fluid-phase starting conditions. Both the bilayer hydrophobic thickness, d_h, and the distance between cholesterol deuterons on each of the monolayers, d_c, may be measured. One obtains $d_h = 26.1 \pm 0.5$ Å, $d_c = 24.6 \pm 0.5$ Å and $d_h = 34.4 \pm 0.5$ Å, $d_c = 30.4 \pm 0.5$ Å for respectively fluid- and gel-phase initial conditions. These values have to be compared to the neutron experimental data, $d_h = 34.6 \pm 0.5$ Å, $d_c = 32.7 \pm 0.5$ Å.

As for pure lipids, a pseudo all-atom picture of the system may be given. Figure 5C shows the system being the closest to the experimental data, that is, that calculated from gel-phase initial conditions. The color code used for pure lipids is also used here, and in addition the cholesterol deuterons are shown as blue spheres. Again the phosphorus layer is well-separated from the glyceroester oxygens and the deuterons of mostly ring A of cholesterol are a little below the phospholipid glycerol backbone, in agreement with neutrons data (Figure 3). Geometrical data and in particular the specific lipid surface from mixed cholesterol−DMPC phases are much more difficult to extract from the simulations due to the presence of two quite different lipids. By defining the unit cell as made of two DMPC molecules plus one cholesterol molecule, one obtains a surface of 141 or 176 Å^2 for bilayers with initial starting conditions respectively in the gel or fluid phase. It is also possible to calculate lateral diffusion parameters for each lipid. For the system run with gel-phase initial conditions, the lateral diffusion parameters are 7.80×10^{-8} cm^2/s for the whole DMPC, 7.50×10^{-8} cm^2/s for cholesterol, and 1.96×10^{-8} cm^2/s for the DMPC polar headgroup. When the initial conditions were those of the DMPC fluid phase, the lateral diffusion constants were 11.7×10^{-8} cm^2/s, 13.9×10^{-8} cm^2/s, and 4.75×10^{-8} cm^2/s for whole DMPC, cholesterol, and the DMPC headgroup, respectively.

The potential hydrogen bonding between the cholesterol OH hydrogen and the oxygens of the carboxyl groups of the DMPC chains was monitored during the entire run. A hydrogen bond is defined when the distance between atoms is within 2 ± 0.5 Å and the O−H−O angle is between 120 and 180°.[38] At the end of the run one determines that, on average over the entire run, there are 4 ± 1 H-bonds with ester oxygens. These figures stand for the entire system; that is to say, there is an average of 25% "carboxyl" H-bond per cholesterol OH. During the course of the entire run, one nonetheless observes that there may be very distinct hydrogen bonding behaviors: most of the potential H-bond distances vary very quickly with time, whereas a few are stable for more than 100 ps. It is also found that the cholesterol hydroxyl is bound to 1 ± 0.1 H_2O.

Discussion

Two major questions were addressed in this work: (i) the vertical location of cholesterol in a membrane and (ii) the capability of molecular mechanics to present structural information on the membrane. The first point is quite clear: cholesterol is well located in the bilayer core, with its OH group in the vicinity of the fatty acyl chain carboxyls, and induces an increase of the membrane hydrophobic thickness. For the second point it has been shown that molecular mechanics can account for membrane structural data and give information about hydrogen bonding, if care is taken in defining adequately the initial conditions of the calculation. All of these aspects will be presented below, the second point being discussed first in order to define which simulation data set is to be taken to discuss cholesterol hydration and hydrogen bonding.

Molecular Mechanics versus Neutron Diffraction. To define a membrane state, one must define both its structure and dynamics. As mentioned in the Introduction, numerous works have been performed on membrane dynamics with or without cholesterol, but to our knowledge there has been no attempt to relate the structural data (hydrophobic thickness, vertical positioning, ...) that may be extracted from the calculation to similar experimental data coming from a method dedicated to structural analysis. Concerning pure phosphocholine membranes in their fluid phase, we have shown herein that the neutron scattering profile calculated from the molecular mechanics coordinates, at the end of a 2 ns run, is in good agreement with the experimental data. In particular the hydrophobic thickness is found to be the same, within the experimental error, giving confidence in the calculation of orientational order parameters from simulations. It has indeed been shown by NMR and neutron scattering that acyl chain order parameters are directly linked to the membrane hydrophobic thickness.[6] The lipid surface, 61 Å^2, and the lateral diffusion constants for DMPC and the DMPC headgroup, 17.0×10^{-8} and 8.80×10^{-8} cm^2/s, respectively, obtained from the fluid-phase simulation compare also very well with experimental values of 61−62 Å^2, 18.0×10^{-8} cm^2/s,[23] and $(7.9-9.3) \times 10^{-8}$ cm^2/s[31] coming from other techniques. All these facts lead to the conclusion that our simulation adequately represents the DMPC fluid phase over 2 ns.

On the other hand, the hydrophobic bilayer thickness, as estimated from a gel-phase simulation of 2 ns, is larger by 3 Å on comparing to the experimental data. This is clearly outside the error limits. It must be mentioned here that the simulation is made at low temperatures (10 °C), which does not favor rapid attainment of equilibrium. However, it is noteworthy that the shapes of the simulation and experimental profiles are very similar, except for the above-mentioned point. The lipid surface, 49 Å^2, and the lateral diffusion constants for DMPC and the DMPC headgroup, 7.1×10^{-8} and 2.1×10^{-8} cm^2/s, respectively, obtained from the gel-phase simulation must also be compared with the experimental values of 48.5−53.8 Å^2 and <0.01 10^{-8} cm^2/s.[23] The calculated lipid surface is within the quite wide range of measured values, but the lateral diffusion constants obtained from simulations are

clearly much higher than the experimental data. It seems thus extremely difficult to "freeze" such a small simulation box, and this appears as a limitation of the simulation technique at least on the few nanosecond time scale of our study. Although the gel phase is incompletely described by the simulation, both the agreements in surface area and in neutron profile line shape let us have confidence in describing correctly a membrane gel phase by molecular dynamics provided longer computational times on larger simulation boxes.

Also of interest are the results with a cholesterol-containing membrane. Here two attempts have been made with two different initial conditions: gel- or fluid-phase DMPC molecules in which one third of phospholipids are substituted by cholesterol molecules. Clearly, the hydrophobic bilayer thickness and the vertical positioning of cholesterol in the membrane, starting from a fluid phase and after a 2 ns run, are in very large disagreement, respectively by 8 and 6 Å, with the neutron data (see Figure 3). Taking an equilibrated fluid-phase phospholipid membrane and embedding cholesterol molecules that are otherwise known to order the membrane[7,19,28,36,43] is therefore not the appropriate way to define the starting conditions. On the contrary, starting from initial gel-phase conditions and after a 3 ns run, the calculation leads to the experimental hydrophobic thickness, within the experimental error. The cholesterol positioning is still underestimated by 2 Å, which is just outside the error limits. The lipid lateral diffusion coefficients obtained from calculations (ca. 8×10^{-8} cm^2/s) are about 1 order of magnitude larger than those experimentally measured by Rand (ca. 10^{-8} cm^2/s)[33] or by Bayerl and co-workers (5×10^{-7} cm^2/s).[14] Again, the values obtained from gel starting conditions are the closest to the experimental data. It must be mentioned that the molecular mechanics box is of finite size and better statistics could be obtained if there were many more molecules in each of the monolayers. Also more computing time would be needed, especially with a very rigid membrane. The results are nevertheless very encouraging and clearly point out that the initial starting conditions for the calculation are of first importance.

Cholesterol Vertical Location in the Membrane. It has been proposed using diffraction methods[12,15,49,50] and spectroscopic techniques[1,7,19,32,41] that cholesterol is entirely located in the membrane. As already mentioned in the Introduction, the accurate vertical location in the membrane has been a little bit controversial. On one hand Worcerster and Franks[49,50] claim that carbon-3 of the steroid skeleton was at 18 Å from the bilayer center of an egg PC membrane, whereas on the other hand Reinl and co-workers[34] proposed that cholesterol could be expelled from the bilayer interior on crossing the former gel-to-fluid transition temperature of pure DPPC. From our study, it is clear that the latter situation is not encountered in cholesterol−DMPC mixtures. Figure 2 clearly shows that the cholesterol location in the membrane is quasi-invariant in the temperature range 10−50 °C, that is, on each side of the main transition temperature of pure DMPC. The center of mass of the six deuterons of [2,2,3,4,4,6-$^2H_6$]cholesterol is located at 16.3 ± 0.5 Å from the bilayer center at 10 °C and 15.1 ± 0.5 Å at 50 °C. This small temperature-induced linear decrease is easily accounted for by the onset of conformational defects that shorten the cholesterol and DMPC chains on increasing the temperature. The distance between cholesterol carbon-3 and the bilayer center has been reported by Worcester and Franks to be 18 Å for cholesterol in egg PC. Adding 0.5 Å to the barycenter of cholesterol deuterons to determine the distance between carbon-3 of the sterol and the membrane center in our DMPC−sterol system leads to 16.8 Å. Because the distribution of egg PC acyl chains is centered on the 18 carbon length, the ∼1−2 Å larger distance found between the cholesterol C-3 position and the bilayer center in egg PC versus DMPC is easily accounted for by the additional carbon bonds of the natural phospholipid.

Cholesterol Location and Bilayer Hydrophobic Thickness. Knowledge of bilayer thickness is of first importance when one wishes to understand biomembrane molecular and mechanical properties. For instance, an increase in bilayer thickness will reduce the passive diffusion of water or neutral solutes across the membrane. On the other hand it has been shown that there is a close relationship between bilayer thickness and the membrane elastic modulus. For instance, in simple systems such as giant vesicles whose membrane is made of phosphatidylcholines, the stiffness of the bilayer is related to the square of the hydrophobic thickness.[11]

The bilayer hydrophobic thickness can readily be measured from the one-dimensional neutron scattering density profiles (as in Figure 1). It can also be estimated from X-ray diffraction methods by performing analogous experiments: the one-dimensional electron density profile is then reconstructed. Wu and co-workers recently demonstrated that bilayer thickness could be measured from the peak-to-peak distance, that is, the distance between the two polar headgroup regions in the electron density profile, with an accuracy of ±0.5 Å if Fourier transformation was performed with more than five orders.[52] In our neutron experiments Fourier transformations could be performed with a number of orders varying from 8 to 10. This leads us to be confident in our measured distances within at least ±0.5 Å. As a verification, the tilt angle of the lipid molecules in the $L_{\beta'}$ phase can be obtained from the DMPC profile at 10 °C, for which $d_h = 32 \pm 0.5$ Å. This tilt angle may be calculated by considering that two tail-to-tail lipid chains in the all-trans conformation span 34.1 Å. Adding two halves of the width (3 ± 0.5 Å) of the glycerolester region[4,6] leads to 37 ± 0.5 Å, and the tilt is then given by $\arccos(32/37) = 30 \pm 1.5°$, which agrees very well with values reported in the literature.[17,23,39]

The net effect of cholesterol is to increase d_h by ∼3−4 Å, independently of temperature. This effect is already well documented in lipid fluid phases. It is indeed common to describe cholesterol as a membrane stabilizer.[5,7,16,19−21,24,27,32,42,48,53] It has also been described as a fluidizing agent[7,19,20] of lipid membranes which are initially in their gel ($L_{\beta'}$ or $P_{\beta'}$) phase in the absence of cholesterol: a liquid-ordered (β) phase is then invoked, which shares the properties of both fluid and gel phases.[25,47] Here we report a 3.5 ± 0.5 Å increase in hydrophobic thickness on going from the $L_{\beta'}$ phase to the β phase which appears at first contradictory with the fluidizing effect mentioned above. However, as already mentioned, lipids are tilted with respect to the membrane normal in this $L_{\beta'}$ phase. Because cholesterol orients perpendicularly to the membrane plane,[7,22] it cancels the phospholipid chain tilt in the β phase. If there was no chain conformational disorder, the bilayer hydrophobic thickness would then be 37.1 Å. Since we measure 36 ± 0.5 Å between the glycerolester regions on each side of the bilayer, at 10 °C, there is indeed a fluidizing effect of cholesterol which results in a bilayer shrinking of 1.1 ± 0.5 Å.

Cholesterol Hydrogen Bonding and Hydration in the Membrane. From neutron scattering, it is found that the center of mass of the six deuterons of cholesterol is 1−2 Å below that of the phospholipid carboxyl oxygens.

This suggests that the hydroxyl group of cholesterol, which is 1.9 Å away from the deuterons' center of mass, has a vertical location at the level of the carboxyl oxygens' barycenter. This reinforces the idea that the cholesterol hydroxyl group is in a favorable position to make hydrogen bonds with the ester oxygens of the phospholipid chains, as also found by simulations. Although molecular dynamics were run in a limited dynamic range, it is nonetheless found that 25% of all cholesterol molecules are potentially engaged in a hydrogen bond with the carboxyl oxygens of phospholipids. Worcester and Franks also favor the hydrogen-bonding hypothesis in a thicker membrane (cholesterol−egg PC). This leads us to suggest that the hydrogen bonding to carboxyl groups may be the leading force responsible for cholesterol vertical positioning in membranes. This is especially interesting with regard to the role of the membrane dynamics regulator assigned to cholesterol in biomembranes. Douliez and co-workers[6] reported that cholesterol almost completely cancels the phospholipid protrusion (out of plane motion) in membranes. Hydrogen bonding between cholesterol and phospholipids would be a good candidate to rationalize such an effect, hence conferring on the sterol the additional role of softener of the membrane surface.

It is also interesting to note that cholesterol is well embedded in the membrane hydrophobic core, which results in a weak hydration, one water molecule per sterol, as reported by an average over 3 ns. It is interesting to relate this finding to that of Faure and co-workers,[10] who studied the hydration of cholesterol in DMPC by means of deuterium NMR of heavy water. They found that 2.3 DMPC molecules plus 1 cholesterol molecule strongly bind 8 water molecules (ordered water) independently of the temperature over the range 10−50 °C. Taking into account our result for cholesterol hydration in the same mixed system, one finds that each DMPC binds ∼3.5 water molecules under these conditions, that is to say about the same number of water molecules as in its pure gel phase (less than 4 H_2O at 10 °C[9]). This clearly reinforces the idea of a well laterally packed bilayer, in the presence of cholesterol.

Conclusion

The use of neutron diffraction and proton−deuterium contrast methods as well as molecular dynamics calculations demonstrated that cholesterol is well embedded in the membrane and occupies a vertical location which favors a hydrogen-bonding interaction between its OH group and the phospholipid fatty acyl chain esters. The temperature invariance of such a location appears to be a good candidate for the regulatory role of cholesterol in membrane dynamics, that is, respectively disordering and ordering lipids that would otherwise be in solidlike or fluidlike phases. Also of interest is the calculation of structural data from molecular dynamics. This allows direct comparison with experiment and points out the limitations of the simulations.

Acknowledgment. The authors wish to thank the ILL in Grenoble and the BENSC in Berlin for grants through the European program "Access to large-scale facilities". Special thanks go to Dr. Thomas Hauss of the HMI for help during experiments in Berlin.

Appendix

Modulus of Structure Factors. Following Saxena and Schoenborn,[37] the hth-order reflection $I(h)$ is related to the corresponding structure factor $F(h)$ by

$$I(h) = L_1(h)\, L_2(h)\, L_3(h)[F(h)]^2 \tag{A1}$$

where $L_1(h) = 1/\sin 2\theta_B$ is the angular velocity term (Lorentz factor), L_2 is a factor correcting for sample mosaicity, for vertical beam divergence, and for a detector not wide enough to receive the entire diffracted beam in the vertical position, and L_3 is a correction for sample absorption and geometry. For calculation of the L_2 factor, we basically follow Saxena and Schoenborn,[37] with the only variance that we calculate the inverse Fourier transform of the product of the Fourier transform of each of the three contributions. This is detailed below for completeness.

(a) Sample Mosaicity. Assuming that it can be modeled by a Gaussian function, the intensity distribution at the detector, in the vertical z direction, may be written as

$$I_M(z) = \sqrt{\frac{4 \ln 2}{\pi \eta^2}} e^{[(4 \ln 2)/(D \sin 2\theta_B \eta)^2](z^2)} \tag{A2}$$

with η the sample mosaicity in degrees, as determined from so-called rocking curves,[37,55] and D the sample-to-detector distance.

(b) Vertical Divergence. Assuming a Gaussian distribution for the beam, one may write

$$I_D(z) = \sqrt{\frac{4 \ln 2}{\pi \epsilon^2}} e^{[(\ln 2)/(D\epsilon)^2](z^2)} \tag{A3}$$

where ϵ is the beam divergence.

(c) Truncation of the Beam by the Slit before the Sample. If the slit height is w, then

$$I_S(z) = I_D(z) \quad \text{for} \quad |z| \le w/2$$
$$I_S(z) = 0 \quad \text{for} \quad |z| > w/2 \tag{A4}$$

The resulting intensity is the convolution of the three terms. For simplicity of calculation, it is better to estimate the Fourier transformation of the final intensity, which is the product of the Fourier transformations of each of the contributions (eqs A2−A4):

$$i(s) = i_0\Big[D \sin(2\theta_B) e^{[(\pi D \sin 2\theta_B \eta)^2/(4 \ln 2)](s^2)} \times D e^{[(\pi D \epsilon_B)^2/(\ln 2)](s^2)} w \frac{\sin \pi w s}{\pi w s}\Big] \tag{A5}$$

Inverse Fourier transformation of the expression between square brackets leads to $L_2(h)$.

$L_3(h)$ corrects for sample absorption and for sample geometry; that is, for higher orders, the sample does not lay entirely in the beam:[30]

$$L_3(h) = \frac{ht(1 - e^{a/h})}{ag(h)}$$

where

$$a = \frac{4\mu t d}{\lambda} \tag{A6}$$

and

$$g(h) = \frac{h\lambda s_w}{2d(b_w + 2/tg\pi b_d)} \quad \text{for} \quad g(h) > 1$$

$g(h) = 1$ otherwise

(i.e. all the sample is in the beam)

In eqs A6 μ is the attenuation factor (5 cm^{-1}), t is the sample thickness (0.0015 cm), b_w and b_d are the beam width (1 cm) and divergence (0.4), s_w is the sample width (7.5 cm), and l is the distance between the last slit and the sample (15 cm).

Sign of Structure Factors. Because of the centrosymmetry of our systems, the structure factors are real and we only need to determine their sign. The method we used takes advantage of the large difference in the neutron scattering length of protons versus deuterons. Because it has been shown that the structure factor, $F(h,\Phi_D)$, determined with a given D_2O content varies linearly with Φ_D, the D_2O volume fraction (% D_2O in H_2O)[30,55] experiments were therefore repeated with at least three hydrating media of variable D_2O content.[49,51,54] Here two methods can be used that we will describe below. The first one (method A) was already described in ref 30, so we will just outline it; the second one (method B), which takes advantage of the linear relationship mentioned above and allows us to predict the sign of the slope on which the $F(h,\Phi_D)$ should align, will be detailed.

(a) Method A.[30] The water scattering density profile, $\rho_w(x)$ can be obtained from the scattering profiles obtained in 100 and 0% D_2O, $\rho_{D_2O}(x)$ and $\rho_{H_2O}(x)$, respectively:

$$\rho_w(x) = \rho_{D_2O}(x) - \rho_{H_2O}(x) \qquad \text{(A7)}$$

which reads in reciprocal space as

$$F_w(h) = F(h,1) - F(h,0) \qquad \text{(A8)}$$

The linear relationship between $F(h,1)$, $F(h,0.5)$, and $F(h,0)$ allows us to determine $|F_w(h)|$. The choice of the absolute sign determination of $F_w(h)$ is made in the following way: the $h = 1$ sign is related to the choice of the origin (it will be (-1) if one sets the origin at the bilayer center); the $h = 2$ sign is related to the sign of the water density profile (-1 if $\rho_w(x)$ is considered as positive); the remaining signs are chosen in order to get a "flat" water distribution at the bilayer center.[30] This latter hypothesis seems to be reasonable when considering membranes where the core is only made of hydrocarbon chains, as in our study. This may not be the case when proteins cross the membrane or make channels.

(b) Method B. The diffraction intensities will linearly increase or decrease on replacing H_2O by D_2O, depending on whether the structure factors are positive or negative, respectively. One may therefore write

$$F(h,\Phi_D) = p(h) + F(h,0) \qquad \text{(A9)}$$

where the slope of the linear variation, $p(h) = F_w(h)$, can be expressed as

$$p(h) = A\int_0^{d_w/2} D_w(x) \cos\left(\frac{2\pi x h}{d}\right) dx \qquad \text{(A10)}$$

where $D_w(x)$ represents the water distribution in the membrane and d_w represents the water layer thickness. In writing eq A10, it is assumed that the origin in x is placed at the center of the water layer. A is a constant depending on the number of water molecules in the unit cell and on the difference between the neutron scattering lengths of the deuteron and the proton. Assuming that the water distribution is to first order, a step function, eq A10 transforms into

$$p(h) = \frac{A}{2}\frac{d}{\pi h d_w}\sin\left(\frac{\pi d_w h}{d}\right) \qquad \text{(A11)}$$

Figure 6 shows plots of eq A11 for three values of d_w/d. It is clearly seen that the slopes $p(h)$ are positive or negative depending on the thickness of the water layer. This figure can be used to determine the signs of $F(h)$. For instance, the slopes of the linear variation of $F(h)$ versus the D_2O content will be positive for the five first orders if $d_w/d < 1/5$. To determine their sign, one will align the structure factors obtained for different D_2O volume fractions on a line of positive slope; for $h = 6$ to 10 one will seek for a negative slope; and so forth. This method will not suffer too much from the possible presence of water in the bilayer

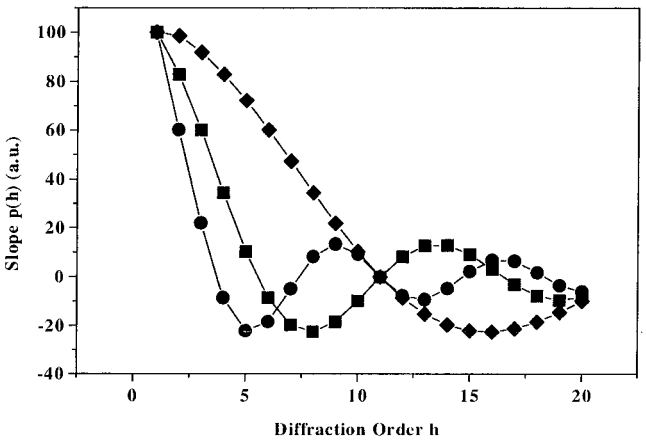

Figure 6. Plot of the slopes, $p(h)$, as a function of diffraction order, h, according to eq A11 of the Appendix. Calculations were made for d_w/d values of 5/55 (◆), 10/55 (■), and 15/55 (●). The slopes of the linear variation of $F(h)$ versus D_2O volume fraction content will be positive for the first 10 (◆), 5 (■), and 3 (●) orders, respectively. See text for details.

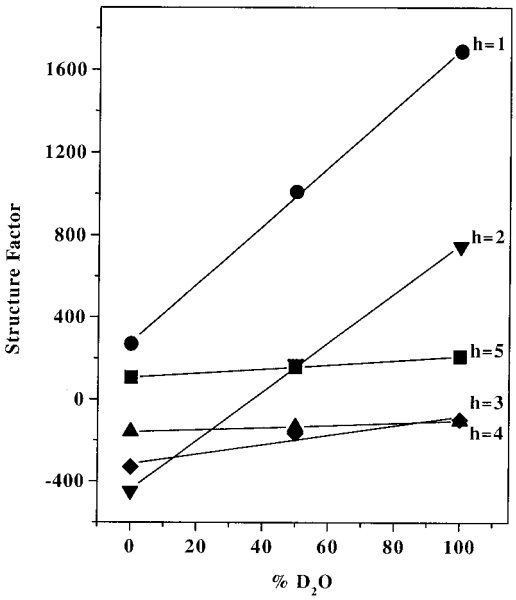

Figure 7. Linear dependence of the experimental structure factors as a function of D_2O volume fraction. The sample is made of DMPC + 30 mol % cholesterol, at 10 °C. Symbols represent the five first diffraction orders; $h = 1$ (●); $h = 2$ (▼); $h = 3$ (◆); $h = 4$ (▲); and $h = 5$ (■). Solid lines are least-squares fits of the experimental values.

core, as opposed to the case for method A, since this contribution will anyway be weaker compared to that for the majority of water located between bilayers. Of course d_w/d must be evaluated. This difficulty can be surmounted in most cases, since d is measured and the bilayer thickness is estimated from knowledge of lipid chain length.

This method has been applied to all our data. As an example, Figure 7 shows the variation of $F(h)$ as a function of D_2O content, for a DMPC sample containing cholesterol, at 10 °C. To build this graph, it has been assumed that $d_w/d < 1/5$, which under our conditions appears to be reasonable, and therefore five positive slopes were searched for. The sequence of signs is therefore (+, −, −, −, +) for $h = 1-5$, respectively. To reconstruct a Fourier profile with the origin at the center of the hydrophobic core, the Redfield rearrangement was performed; that is, every odd structure factor was negated. The sequence of signs then becomes (−, −, +, −, −), as found in Table 1.

It must be mentioned here that method A was also applied to our data and gave the same sign sequence. One will nonetheless prefer method B because the criterion of a "flat" water profile in the bilayer core is somewhat difficult to quantify.

LA001382P